HIV-1 Amplifies IL-8 Response Of Human Stellate Cells To Gram-Positive Microbial Products Via H4K5 Histone Acetylation

Lumin Zhang[1]*, Rabab O. Ali[1]*, Naichaya Chamroonkul[5], Parissa Tabrizian[2], Myron Schwartz[2], Ganesh Gunasekaran[2], Thomas Schiano[3], Maria Isabel Fiel[4], Steven Ward[4], Meena B. Bansal[1]

[1]Department of Medicine, Icahn School of Medicine at Mount Sinai, New York, NY, USA

[2]Department of Surgery, Icahn School of Medicine at Mount Sinai, New York, NY, USA.

[3]Recanti-Miler Transplant Institute, Icahn School of Medicine at Mount Sinai, New York, NY, USA.

[4]Department of Pathology, Icahn School of Medicine at Mount Sinai, New York, NY, USA.

[5]Gastroenterology and Hepatology Unit, Division of Internal Medicine, Faculty of Medicine, Prince of Songkla University, Hatyai, Songkhla, Thailand

*The authors contribute equally to this work

Corresponding Author

Meena B. Bansal, MD, Icahn School of Medicine at Mount Sinai, 1425 Madison Avenue, Room 11-70; Box 1123, New York, NY 10029, E-mail: meena.bansal@mssm.edu, Fax: 212-849-2574, Tel : 212-659-9510.

Financial support

This work was supported by research grant NIH R56DK92128 and R01DK108364 to MBB

Abstract

Background: Patients living with Human Immunodeficiency Virus (PLWH) develop accelerated liver fibrosis, but the exact mechanism remains unknown. Hepatic stellate cell (HSC) activation is the cornerstone for liver fibrosis and influenced by multiple factors, such as viral infection, hepatocellular injury, chronic immune activation, gut mucosal barrier dysfunction, and microbial translocation. Unlike gram-negative bacterial products, the impact of gram-positive microbial products in Human Immunodeficiency Virus 1 (HIV-1) associated liver inflammation and fibrosis remains poorly understood. In this study, we investigated the effect of lipoteichoic acid (LTA), a major gram-positive bacterial component, on HSCs in the context of HIV-1 infection. **Methods:** Human HSCs were isolated from the livers of both non-HIV and HIV-infected patients undergoing hepatic resection. The inflammatory responses of HSCs to LTA stimulation were measured by ELISA before or after HIV-1BaL ex vivo expision. Western blotting, ChIP-qPCR and RNA-seq were used to reveal the mechanisms contributing to the IL-8 response to LTA stimulation and HIV-1BaL exposure in HSCs. **Results:** While LTA stimulation modestly increased IL-8 production in HSCs, this effect was significantly amplified in HIV-1-infected HSCs. Elevated IL-8 levels were detected in HIV-1+ liver sections, and IL-8 treatment of cultured HSCs significantly increased α-SMA and COL1A1 expression, supporting IL-8 as a key inflammatory driver of liver fibrosis in HIV-1^+ individuals. Transcriptomic analyses implicated histone acetylation as a regulator of the enhanced IL-8 response of HSCs to LTA in HIV-1 infection. Consistent with this, treatment with Trichostatin A (TSA), a histone deacetylase (HDAC) inhibitor, further increased the IL-8 response in HIV-1-infected HSCs. ChIP-qPCR confirmed that histone H4K5 acetylation facilitated IL-8 promoter transactivation, rendering HIV-1-infected cells more responsive to LTA. **Conclusions:** HIV-1 infection sensitizes HSCs to LTA stimulation, leading to an amplified IL-8 response mediated through histone acetylation that may accelerate liver fibrosis progression in PLWH. As microbial translocation persists despite effective antiretroviral

therapy, these findings underscore the need for targeted strategies to mitigate liver fibrosis in HIV-1 infected HIV-1^{+} individuals.

Abstract Word Count: 318

Keywords

Human Immunodeficiency Virus, LTA, Inflammatory response, Fibrosis, Hepatic Stellate Cells, Microbial Translocation

Abbreviations

Antiretroviral therapy (ART), Bovine serum albumin (BSA), Chromatin immunoprecipitation with quantitative PCR (ChIP-qPCR), Cycle threshold (CT), C-C chemokine receptor type 5 (CCR5), C-X-C motif chemokine receptor 1 (CXCR), Differentially expressed genes (DEGs), Dulbecco's Modified Eagle Medium (DMEM), Enzyme-linked immunosorbent assay (ELISA), Hepatic stellate cells (HSC), Hepatitis B Virus (HBV), Hepatitis C Virus (HCV), Histone deacetylase (HDAC), Human Immunodeficiency Virus 1 (HIV-1), Immunohistochemistry (IHC), Interleukin-1β (IL-1β), Interleukin-8/CXCL8 (IL-8), Lipopolysaccharide (LPS), Lipoteichoic acid (LTA), Multiplicity of infection (MOI), Pathogen-associated molecular pattern (PAMP), Primary HSCs (pHSCs), Persons living with HIV (PLWH), RNA sequencing (RNA-seq), Sirtuin (SRT), Toll-Like Receptor (TLR), Trichostatin A (TSA), Transcription factor (TF), Tumor necrosis factor α (TNF-α), and Weighted Gene Co-Expression Network Analysis (WGCNA), Body Mass Index (BMI), Liver Stiffness Measurement (LSM), Platelet count (Plt), Aspartate Aminotransferase (AST), Alanine Aminotransferase (ALT), Alkaline Phosphatase (ALP), Albumin (Alb), Fasting Blood Sugar (FBS), Total cholesterol level (Chol), Triglycerides (TG), High-Density Lipoprotein (HDL), Low-Density Lipoprotein (LDL), Controlled Attenuation Parameter (CAP), Hepatic Steatosis Index (HIS), Fibrosis-4 Index (FIB-4).

Introduction

Human immunodeficiency virus 1 (HIV-1) infection is characterized by severe depletion of CD4+ T cells, leading to attenuated systemic immunity. Consequently, individuals living with HIV-1 experience increased susceptibility to opportunistic bacterial infections and community-acquired infections. For instance, the risk of *Streptococcus pneumoniae* infection is 100 times higher in HIV-positive individuals than in the general population[1]. Early during HIV infection, the depletion of gut associated CD4+ T cells disrupts the integrity of the intestinal barrier, facilitating microbial products translocation into the peripheral circulation[2]. Notably, microbial translocation remains elevated even in patients undergoing with antiretroviral therapy (ART), as ART does not restore gut permeability. Thus, microbial translocation has been identified as a major driver of sustained systemic immune activation in patients living with HIV (PLWH).

HIV-induced damage to the gastrointestinal mucosa leads to the translocation of both gram-positive and gram-negative microbial products from the gut lumen into the liver via the portal vein[3]. Although translocation of gram-negative bacterial products occurs more efficiently following mucosal injury[4], clinically relevant gram-positive bacteria can also frequently enter the peripheral circulation[5], either through shared routes or opportunistic infections. While extensive studies have addressed the impact of gram-negative microbial products, such as lipopolysaccharide (LPS), on chronic immune activation, liver injury and fibrogenesis in HIV infection[6,7], the role of gram-positive microbial products remains poor understudied. Lipoteichoic acid (LTA), a major component of the gram-positive bacterial cell walls, is recognized as pathogen-associated molecular pattern (PAMP) capable of significantly modulating the host immune immunity[8-10]. Functionally similar to LPS, LTA induces CD14-dependent nitric oxide release from vascular smooth muscle cells, macrophages, and mononuclear cells[11]. Recent studies have showed high serum LTA levels in HIV-positive individuals, associated with increased autoantibody secretion and enhanced immune responses[12]. Given the liver's unique

position as the first organ to interact with gut-derived microbial products via portal circulation, elucidating the influence of LTA on liver cells , particularly hepatic stellate cells (HSCs), in HIV associated chronic liver disease is critical but. remains inadequately explored.

End-stage liver disease contributes to represent a significant cause of mortality among HIV-positive individuals despite effective ART, underscoring the persistent impact of HIV in liver dysfunction and progressive fibrosis[13]. Several studies have established a positive correlation between HIV RNA levels and advanced fibrosis in HIV mono-infected patient[14-16]. Furthermore, HIV-1 co-infection with Hepatitis C Virus (HCV) accelerates liver fibrosis progression by threefold compared to HCV mono-infection[17]. Although interactions between HSCs and liver macrophages are crucial for HSC activation[18], HSCs remain central drivers of hepatic fibrogenesis. Our previous studies[19,20] have shown that HIV-1 infection enhances the inflammatory responses of liver macrophages to gram-negative microbial products, such as LPS, resulting in elevated pro-inflammatory cytokine production including Interleukin-8/CXCL8 (IL-8). However, the contributions of these cytokines to direct HSC activation require further clarification.

In this study, we investigated the inflammatory responses of primary human HSCs isolated from HIV-1 negative and HIV-1 positive individuals upon LTA stimulation. Our results demonstrated that HIV-1 infection amplifies IL-8 responses to LTA stimulation in HSCs, and hepatic IL-8 directly exhibits pro-fibrogenic effects at the transcriptional level in HIV-1 positive liver tissues. Additionally, we found histone acetylation, specifically H4K5 acetylation, mediates the transactivation of IL-8 in HIV-1-infected HSCs, providing new mechanistic insights into HIV related liver fibrosis.

Materials and Methods

Ethics Statements

De-identified liver resection specimens from HIV-1+ individuals (n=7) were provided by Drs. Schwartz, Ganeskaran, and Fiel. In all cases, HIV was effectively suppressed with ART. Normal liver tissue obtained from the Mount Sinai Biobank served as controls (HIV non-infected liver tissues i.e., controls, n=10 with 9 from individuals undergoing resection for colon cancer metastases, and 1 from a cholangiocarcinoma patient, n=10). Liver tissue samples were obtained from patients undergoing clinical liver transplantation or tumor resection. Tissues were formalin-fixed, frozen, or placed in Dulbecco's Modified Eagle Medium (DMEM). These studies have been approved by Mount Sinai IRB (GCO #06-0523 and #10-1211). Tissues from non-infected and HIV infected individuals were utilized for immunohistochemistry (IHC) staining of IL-8. Blood samples were separately collected from HIV+ participants enrolled in a nonalcoholic fatty liver disease (NAFLD) study. The characteristics of the study population in Table 2 are analyzed by R package survey[21] and tableone[22].

Isolation of Human Stellate Cells from HIV Non-infected and HIV-1 Infected Liver tissues

Primary HSCs (pHSCs) were isolated from surgical resection specimens by performing collagenase perfusion and mincing of the liver tissue. Cells were washed with PBS four times and pelleted at 300 x G for 5 min. Cells were then re-suspended in DMEM followed by gradient centrifugation using 25 and 50% Percoll (Pharmacia, Uppsala, Sweden), as described[23]. pHSCs were enriched by adherence to tissue culture plates. After two weeks in culture, α-SMA immunostaining was used to check the purity of pHSCs.

Tissue Immunohistochemistry Assay

The liver tissue sections were prepared in duplicate for each patient. After rehydrated and treated for antigen retrieval, slides were incubated with anti-human IL-8 antibody (NOVUS, Cat

No NBP2-33819, 1:200 dilution) overnight at 4°C in a humidified chamber. The staining was performed using ImmPress™ Duet Double staining polymer kit (Cat. MP-7724). Four random visual areas were selected for each tissue section. The images were captured with Zen software for LSM 880 laser air-scanning microscope (magnification: 100x). IL-8 signal intensity was quantified by Fiji image J software (NIH, Bethesda, MD).

Flow Cytometry Analyses

CXCR1, CXCR2, and TLR2 expression in pHSCs was evaluated before and after gp120 stimulation (100ng/ml). Cells were re-suspended in PBS containing 0.5% bovine serum albumin (BSA) at concentration 0.5- 1×10^6 cells/ml. incubated Fc-R blocking reagent, and stained with anti-human CXCR1-APC (Biolegend, Cat No 320612), CXCR2-FITC (Biolegend, Cat No 320704), and TLR2-PE (Biolegend, Cat No 309708) for 15 min. After fixation and permeabilization at 4^0C for 20 min, samples were analyzed on LSRII (BD Biosciences). Data was analyzed using FCS express 6 software (De Novo software).

Histone Protein Extraction and Acetylation Protein ELISA

$1x10^6$ pHSCs cells and Lx2 were seeded in 10 cm dishes and infected with HIV-1_{BaL} virus (NIH AIDS Reagent program, Bethesda, MD) for 48 hrs. Total histone proteins were extracted by EpiQuickTM total Histone extraction Kit (Cat. OP-0006) as per manufacturer instructions. 200 ng of histone protein was subjected to acetylation protein quantification using a histone acetylation ELISA kit (Cat. P-4022-96) following manufacturer instructions.

RNA Extraction and RT-qPCR

Total RNA was extracted by using RNeasy spin columns (Qiagen, Cat No:74136). After treatment with RNase-free DNase (Qiagen, Chatsworth, CA), RT was performed on RNA by using Clontech RNA to cDNA EcoDry kit according to the manufacturer's protocol. RT-qPCR

was performed on Roche Lightcycle II 480. Reactions were carried out in 10 μL by using SYBR Green PCR master mix according to the manufacturer's protocol (Bio-Rad, Cat No: 1708884). The concentration of primer pairs was 300 nM. All primer sequences are shown in Table 1. All reactions were performed in triplicate. To make comparisons between samples and controls, the cycle threshold (CT), defined as the cycle number at which the fluorescence is above the fixed threshold values were normalized to the CT of α-actin in each sample.

IL-8 ELISA Assay

Isolated HSCs were treated with different conditions for 24 hrs. IL-8 production in the supernatant was collected at indicated time and measured by using human IL-8 ELISA Kit (Affymetrix, Cat No: 88-8086-88) according to the manufacturer's protocol.

CHIP RT-PCR Assay

1x10^6 pHSCs cells were infected with HIV-1_{BaL} virus (NIH AIDS Reagent program, Bethesda, MD) for 48 hrs. Chromatin fragments were prepared with EZ-ZymeTM Chromatin Prep Kit (Cat. 17-375). Then CHIP assay was performed using Magna CHIPTM G chromatin immunoprecipitation Kits (Cat. 17409). After DNA purification, IL-8 promoter activation was examined by SYBR Green RT-PCR. CHIP-seq was analyzed using a pipeline of bowtie2[24], macs callpeak[25], samtools[26], bedtools[27], and deeptools[28]. H4K5 peaks in CXCL8 were visualized using IGV tools.

RNA-Seq Analysis

Total RNA was extracted from Lx2 cells treated with Medium, HIV-1_{BaL} virus (MOI=0.1) and/or LTA (1ug/ml) (n=3 for each). RNA quality was assessed by a Nano Drop 2000 Bioanalyzer, and RNA-Seq was performed by Mount Sinai NGS core facility. RNA-Seq analysis was performed using a pipeline of STAR[29], htseq[30], Deseq2[31] with batch adjustment, and hg19 annotation.

Pathway analysis of RNA-seq was conducted using Cytoscape with ClueGO 14 and R packages: clusterProfiler[32], enrichplot[33], and Weighted Gene Co-Expression Network Analysis (WGCNA)[34].

Western Blot

Tissue proteins from livers tissue samples from HIV non-infected controls and HIV-1 mono-infected individuals were purified with T-PER Tissue protein Extraction Reagent (Thermo , Cat No:78510). Equal amounts of protein were loaded in each lane for NuPAGE 4-12% Bis-tris gel and then transferred to polyvinylidene difluoride membranes. The membranes were washed with blotting buffer (1× PBS containing 0.1% Tween20) and then blocked for 60 min in blotting buffer containing 10% low-fat powdered milk. Membranes were washed 3 times with blotting buffer, incubated at 4^0 C overnight with primary antibody (1:1000) containing 5% lowfat powdered milk, and incubated with secondary antibody (1:1000) at room temperature for 60 min. Target proteins were developed with TMB 1-component membrane solution (SeraCare Life Sciences Inc., Milford, MA). α-SMA (NOVUS, Cat No. NBP 1-45433 and NB100-56565), Collagen I (NOVUS, Cat No: NBP 2-12446), MMP9 was purchased from Navius Bio. GAPDH was purchased from Santa Cruz Biotechnology (Santa Cruz, Cat No. sc-66163). The blots were detected with Amersham Imager 600 system. The relative expression of proteins was normalized to beta-actin and analyzed using Image J.

Statistical Analysis

Data are presented as means ± standard error (SEM). Statistical analysis was evaluated by GraphPad Prism 5.0 (La Jolla, CA). Comparisons between two groups were made using parametric (Student's *t* test) or nonparametric (Wilcoxon signed ranks test) statistical tests, as appropriate. One-way ANOVA with Kruskal-Wallis test was used to compare multiple groups. For immunostaining, co-localization was analyzed by Fiji image J software (NIH,

Bethesda, MD) and presented using Pearson's R value. P values of <0.05 were considered statistically significant and 0.05-0.09 as trending towards significance. Unless otherwise specified, non-significant results indicate $p \geq 0.1$.

Results

HIV-1_{BaL} exposition Increases IL-8 Response of pHSCs to LTA Stimulation

To evaluate the effect of lipoteichoic acid (LTA) stimulation on primary human hepatic stellate cells (pHSCs), three pHSCs lines were isolated from human liver tissues without HIV-1 infection (control pHSCs). Control pHSCs were stimulated with LTA, and the secretion of pro-inflammatory cytokines IL-6, IL-8, IL-10, and TNF-α was measured both before and post HIV-1_{BaL} exposition for 48 hours. No significant induction of IL-6, TNF-α, or IL-10 was observed following LTA treatment of control pHSCs, either with or without HIV-1_{BaL} exposure (Supplemental Figure 1). However, 48 hours post-HIV-1_{BaL} exposure, LTA stimulation significantly increased the release of IL-8 from control pHSCs (Figure 1A), compared to control pHSCs stimulated with LTA alone.

To validate these findings, IL-8 secretion was measured following LTA stimulation in pHSCs isolated from HIV-1-infected liver tissues (HIV^+ pHSCs). Two out of three HIV+ pHSCs exhibited significantly increased IL-8 secretion upon LTA stimulation (Figure 1B). Consistent with these findings, when Lx2 cells were co-stimulated with LTA and HIV-1_{BaL}, a synergistic increase in IL-8 secretion was observed (Figure 1C).

HIV-1_{BaL} infection in Lx2 cells could be effectively suppressed by the C-C chemokine receptor type 5 (CCR5) antagonist Maraviroc, leading to a subsequent reduction in p24 levels in cell

supernatant (Figure 1D). Also, maraviroc pre-treatment significantly reduced the enhanced IL-8 response to LTA stimulation in HIV-1_{BaL} exposition Lx2 cells (Figure 1E).

To explore the mechanism underlying IL-8 secretion from HSCs stimulated by LTA, we assessed cell surface receptor expression, including IL-8 receptors (C-X-C motif chemokine receptors, CXCR1 and CXCR2) and the LTA ligand receptor (Toll-Like Receptor 2, TLR2) by flow cytometry before and after control pHSCs stimulated with gp120, an HIV-1 envelope protein. Only CXCR1 expression was upregulated following gp120 stimulation, whereas CXCR2 and TLR2 expression remained unchanged (Figure 2A). An IL-8 inhibitor failed to suppress IL-8 secretion in response to LTA stimulation (Figure 2B). Furthermore, treatment of Lx2 cells with an IL-8 receptor inhibitor or a TLR2 inhibitor did not reverse the HIV-1_{BaL}-enhanced IL-8 secretion upon LTA stimulation (Figure 2C).

Collectively, these findings suggest that HIV-1 infection may sensitize the primary human HSCs to LTA stimulation, promoting increased IL-8 secretion through a pathway independent of a IL8 receptor/TLR2 signaling.

IL-8 Expression is Elevated in HIV-1-Infected Human Liver Tissue

To further validate these findings, we analyzed the mRNA expression levels of pro-inflammatory and fibrogenesis markers in liver tissues from PLWH. Liver tissues from PLWH exhibited increased mRNA expression of IL-8, TGF-β and α-SMA compared to liver tissues from HIV-1 negative individuals (Figure 3A). Similarly, α-SMA protein expression was elevated in HIV-1-infected liver tissues compared to controls (Figure 3B). Immunohistochemical (IHC) staining analysis confirmed increased hepatic IL-8 expression in HIV-1 infected liver tissues compared to HIV-1-negative liver tissues (Figure 3C). Moreover, ELISA data using serum from HIV^+ individuals showed that individuals with HIV-1 viremia and liver fibrosis had significantly higher

IL-8 levels than those of aviremic individuals and viremic individuals without liver fibrosis. Although there was no difference in serum LTA levels between individuals stratified by HIV-1 viremia and liver fibrosis, individuals with both HIV-1 viremia and liver fibrosis exhibited markedly higher serum LTA concentrations (mean = 138.81 pg/ml), compared to those with either liver fibrosis only (mean = 96.44 pg/ml) or those negative for both HIV-1 viremia and liver fibrosis (mean = 19.28 pg/ml) (Figure 3D). These findings reinforce the role of IL-8 in liver fibrosis associated with HIV-1 infection.

To investigate whether LTA and/or IL-8 have direct pro-fibrogenic effects, we treated Lx2 cells with varying doses of LTA and IL-8. RT-PCR results revealed that LTA stimulation increased IL-8 gene expression with a dose-dependent manner and without significantly affecting other pro-fibrogenic genes in Lx2 cells (Figure 4A). Treatment with IL-8 repeatedly increased the protein levels of pro-fibrogenic markers α-SMA and Collagen I in Lx2 cells (Figure 4B).

Collectively, these results underscore the potential pathological relevance of IL-8 response to LTA in hepatic fibrosis in the context of HIV-1 infection.

RNA-seq Suggests Post-translational Regulation of Hepatic IL-8 Response to LTA in HIV-1 Infection

To clarify how HIV-1 exposition primes HSCs for IL-8 response upon LTA exposition, we conducted RNA sequencing (RNA-seq) analysis of Lx2 cells under three conditions: untreated, exposed to HIV-1_{BaL} alone, and co-exposed to HIV-1_{BaL} plus LTA (Figure 5). Although statistical significance was not reached in differential gene expression analysis (Figure 5A-B), IL-8 trended higher in cells co-stimulated with HIV-1_{BaL} and LTA compared to untreated Lx2 cells, or Lx2 cells exposed with HIV-1_{BaL} alone (p=0.059) (Figure 5C).

using WGCNA analysis, differentially expressed genes (DEGs) correlated with IL-8 (correlation coefficient >0.2, $p \leq 0.05$) were analyzed by Cytoscape using ClueGO, revealing enrichment of the tRNA aminoacylation (Figure 5D-E). Notably, Sirtuin 4 (SIRT4) was upregulated (Figure 5F), whereas Sirtuin3 and the other aminoacylation related genes were relatively reduced. Given the role of SIRT3 and SIRT4 in regulating protein acetylation and deacetylation under the conditions of oxidative stress and inflammation[35], we further check other acetylation related genes. RNA-seq analysis identified that genes associated with histone H4 acetylation and deacetylation—such as HDAC2 and MORFL2[36,37]—were significantly regulated by the combined exposed to HIV-1_{BaL} and LTA (Figure 5G), indicating a histone acetylation potential involved in enhanced expression of IL-8 in HIV-1 exposed Lx2 cells [35].

H4K5 Acetylation is Essential for IL-8 Transactivation in HIV-1 exposed HSCs

To investigate the role of histone acetylation in the HIV-1-mediated IL-8 response to LTA in HSCs, we assessed IL-8 response in the presence of HDAC inhibitor, Trichostatin A (TSA). TSA significantly increased IL-8 secretion in response to LTA stimulation in both normal HSCs (Figure 6A) and HIV-1+ pHSCs (Figure 6B), specifically without affecting the production of IL-1β, TNF-α, IL-6, or IL-10 (Supplemental Figure 1). Furthermore, HIV-1_{BaL} infection increased total acetylation levels in Lx2 cells (Supplemental Figure 2). Among the histone acetylation measured, H4K5 acetylation levels were significantly elevated (Figure 6C), which was confirmed by western blot results (Figure 6D). Additionally, no significant changes were observed in H3 acetylation (Supplemental Figure 3A-D).

CHIP-RT-PCR analysis demonstrated H4K5 acetylation at the IL-8 promoter in HIV-1 infected Lx2 cells, with enrichment at NFκB, AP-1, and NF-IL16 binding sites (Figure 6E-F). In line with this, CHIP-seq peaks in NF-kB and AP-1 binding motifs near IL-8(CXCL8) transcriptional start sites confirmed these observations (Supplementary Figure 4A- B).

Collectively, these results show that H4K5 acetylation at the IL-8 promoter is crucial for IL-8 transactivation in response to LTA stimulation in HIV-1 infected hepatic stellate cells.

Discussion

End-stage liver disease is a leading cause of mortality in HIV-infected individuals, with several studies confirming a positive correlation between HIV viremia and advanced fibrosis in HIV mono-infection[13-16]. Chronic HIV infection can disrupt host immune homeostasis and accelerates liver fibrosis, yet the mechanisms by which HIV-mediated inflammation contributes to hepatic fibrogenesis remain unclear. Our *ex vivo* and *in vitro* analyses suggest that HIV-1-exposition of hepatic stellate cells (HSCs) amplify their IL-8 response to a gram-positive microbial product known as lipoteichoic acid (LTA). We identified histone acetylation-mediated transactivation of IL-8 in HSCs as a key mechanism in this process.

Elevated serum IL-8 levels (≥46.5 pg/ml) are strongly associated with liver-related mortality and liver transplantation[38,39]. While studies have shown increased IL-8 levels in HIV mono-infection[40], the pathological role of IL-8 in HIV associated liver fibrosis remains unclear. Serological studies reported no correlation between IL-8 levels and liver fibrosis in HIV/HCV co-infection, whereas other studies suggest that elevated IL-8 can predict 3-year risk of fibrosis in HIV/HCV co-infection[41,42]. In our cohort of HIV-1 positive individuals without HCV co-infection, serum IL-8 levels were significantly higher in viremic individuals with advanced fibrosis compared to non-viremic individuals. Serum IL-8 levels differed by viremic status only among HIV-1+ individuals with advanced fibrosis, suggesting a direct correlation between IL-8 expression and HIV-1 related pathogenesis during advanced fibrosis. Immunohistochemical analysis of HIV-1-infected liver tissues confirmed increased hepatic IL-8 expression alongside enhanced pro-fibrogenic gene expression (α-SMA and collagen I). Furthermore, *in vitro* analysis of stellate cell lines

demonstrated that IL-8 contributes directly to liver fibrosis by inducing pro-fibrogenic gene expression in HSCs.

Similarly, studies on TNF-α pre-incubated HSCs suggest that IL-8 serves as a marker of acute inflammatory response to liver injury by activated HSCs[43,44]. Moreover, when HSCs were primed with TNF-alpha and IL-1, subsequent LTA stimulation significantly induced IL-8 production through enhanced NF-kB activation [45]. In our study, without pre-treatment with TNF-α and IL-1β, LTA exposure still led to increased IL-8 secretion from HSCs, an effect amplified in the presence of HIV-1. Importantly, no induction of TNF-α and IL-1β was observed in HIV-1 exposed HSCs, underscoring the role of HIV in modulating HSCs' response to gram-positive microbial products. Although the previous study have suggested that interactions among HIV-1, immune cells/mediators, and HSCs via TLR pathway[46], our data demonstrate that exaggerated IL-8 response to LTA in HIV-1 infected HSCs is independent of IL-8 receptors and TLR2 mediated pathways. Notably, RNA-seq results of Lx2 cells co-exposed to HIV-1 and LTA revealed no activation of the canonical NF-κB signaling pathway in IL-8 induction (Supplementary Figure 5), implying the involvement of an alternative transcriptional mechanism contributing to IL-8 induction.

Our further transcriptomic analysis uncovered a correlation between the aminoacylation pathway and IL8 transactivation. RNA-seq analysis also identified that genes related to H4 acetylation were significantly modulated upon co-exposition to HIV-1 and LTA. IL-8 promoter methylation and acetylation has been implicated in the post-translational regulation of IL-8 activation[47]. Moreover, IL-8-driven chronic inflammation in various pathological conditions can be reversed via acetylation inhibition by Histone deacetylases (HDACs)[48]. Our ex vivo experiments using TSA to induce histone acetylation in HSCs specifically increased IL-8 response to LTA stimulation irrespective of HIV-1 exposition, while no effects on the induction of

IL-6, IL1beta and TNF production. Examinations by using ELISA, CHIP-seq and ChIP-qPCR, we identified increased histone acetylation, specifically H4K5 acetylation, at the IL-8 promoter during HIV-1 infection. This H4K5 facilitates chromatin remodeling and recruitment of the three most critical binding sites in the IL-8 promoter i.e., transcription factors AP-1, NF-IL-6, and NF-kB[49]. These findings align with observations in other diseases, such as cystic fibrosis where histone hyperacetylation through use of histone deacetylase (HDAC) inhibitors promotes IL-8 transcription[50-53].Similarly, histone hyperacetylation promotes IL-8 transcription in hepatitis B virus (HBV) infection, inducing an amplified IL-8 response to HBV replication in HepG2 cells[54]. The unique role of histone acetylation in modulating HSCs responses to microbial products in HIV-associated liver disease has not been previously explored and warrants further investigation. Our study is the first to suggest a direct role of IL-8 in HIV-1-associated HSCs activation and liver fibrosis.

Conclusion

In conclusion, our *ex vivo* and *in vitro* analyses highlight the pathological significance of LTA in hepatic inflammation and fibrogenesis during chronic HIV-1 infection. Elevated serum LTA levels in HIV-1 individuals with fibrosis and viremia, coupled with an enhanced IL-8 response to LTA in HSCs under HIV-1 exposure, underscore the critical role of gram-positive microbial products in HIV associated chronic liver disease. Mechanistic insights from transcriptomic analysis revealed that HIV-1 infection enhances histone H4K5 acetylation, amplifying the IL-8 response to LTA stimulation in HSCs. Analysis of liver tissues from HIV-1+ individuals illustrated this exaggerated pro-inflammatory response of HSCs to LTA as direct pro-fibrogenic effects via hepatic IL-8. Our findings advance understanding of liver fibrosis pathogenesis in HIV by linking gut-derived microbial products, HSC activation, and IL-8 secretion via histone acetylation, presenting important pathological and therapeutic implications for HIV-associated liver fibrosis.

Acknowledgement

We appreciate the reagents support from NIH AIDS Reagents Program.

Author's Contribution

Dr. Lumin Zhang and Dr. Meena B. Bansal conceptualized and designed the experiments. Dr. Lumin Zhang performed the experiments and conducted bioinformatics analyses. Dr. Naichaya Chamroonkul prepared serum samples. Dr. Lumin Zhang, Dr. Rabab O. Ali, and Dr. Meena B. Bansal analyzed the data and drafted the manuscript. Dr. Parissa Tabrizian, Dr. Myron Schwartz, Dr. Ganesh Gunasekaran, Dr. Thomas Schiano, and Dr. Maria Isabel Fiel provided clinical samples and associated clinical data. All authors contributed to manuscript revisions and approved the final version.

Funding

This work was supported by research grant NIH R56DK92128 and R01DK108364 to MBB

Conflict of Interest

The authors declare no conflicts of interest.

Data availability

Processed data files are available at github.com/lumin2003/HIV_LTA_files/

Declarations

The human study has been approved by Mount Sinai IRB (GCO #06-0523 and #10-1211).

Consent for publication

No individual patient information in this study.

Competing interests

All the authors have no competing interests in this study.

References

References

Uncategorized References

1 Zhang, L. *et al.* Humoral immune responses to Streptococcus pneumoniae in the setting of HIV-1 infection. *Vaccine* **33**, 4430-4436 (2015). https://doi.org/10.1016/j.vaccine.2015.06.077

2 Sandler, N. G. & Douek, D. C. Microbial translocation in HIV infection: causes, consequences and treatment opportunities. *Nat Rev Microbiol* **10**, 655-666 (2012). https://doi.org/10.1038/nrmicro2848

3 Ipp, H., Zemlin, A. E., Erasmus, R. T. & Glashoff, R. H. Role of inflammation in HIV-1 disease progression and prognosis. *Crit Rev Clin Lab Sci* **51**, 98-111 (2014). https://doi.org/10.3109/10408363.2013.865702

4 Ljungdahl, M. *et al.* Bacterial translocation in experimental shock is dependent on the strains in the intestinal flora. *Scand J Gastroenterol* **35**, 389-397 (2000). https://doi.org/10.1080/003655200750023958

5 Dillon, S. M., Frank, D. N. & Wilson, C. C. The gut microbiome and HIV-1 pathogenesis: a two-way street. *AIDS* **30**, 2737-2751 (2016). https://doi.org/10.1097/QAD.0000000000001289

6 Kaspar, M. B. & Sterling, R. K. Mechanisms of liver disease in patients infected with HIV. *BMJ Open Gastroenterol* **4**, e000166 (2017). https://doi.org/10.1136/bmjgast-2017-000166

7 Debes, J. D., Bohjanen, P. R. & Boonstra, A. Mechanisms of Accelerated Liver Fibrosis Progression during HIV Infection. *J Clin Transl Hepatol* **4**, 328-335 (2016). https://doi.org/10.14218/JCTH.2016.00034

8 Ginsburg, I. Role of lipoteichoic acid in infection and inflammation. *Lancet Infect Dis* **2**, 171-179 (2002). https://doi.org/10.1016/s1473-3099(02)00226-8

9 Weidenmaier, C. & Peschel, A. Teichoic acids and related cell-wall glycopolymers in Gram-positive physiology and host interactions. *Nat Rev Microbiol* **6**, 276-287 (2008). https://doi.org/10.1038/nrmicro1861

10 Theilacker, C. *et al.* Protection against Staphylococcus aureus by antibody to the polyglycerolphosphate backbone of heterologous lipoteichoic acid. *J Infect Dis* **205**, 1076-1085 (2012). https://doi.org/10.1093/infdis/jis022

11 Hattor, Y., Kasai, K., Akimoto, K. & Thiemermann, C. Induction of NO synthesis by lipoteichoic acid from Staphylococcus aureus in J774 macrophages: involvement of a CD14-dependent pathway. *Biochem Biophys Res Commun* **233**, 375-379 (1997). https://doi.org/10.1006/bbrc.1997.6462

12 Siewe, B., Keshavarzian, A., French, A., Demarais, P. & Landay, A. A role for TLR signaling during B cell activation in antiretroviral-treated HIV individuals. *AIDS Res Hum Retroviruses* **29**, 1353-1360 (2013). https://doi.org/10.1089/AID.2013.0115

13 Sanmartin, R. *et al.* Progression of liver fibrosis in HIV/hepatitis C virus-coinfected individuals on antiretroviral therapy with early stages of liver fibrosis at baseline. *HIV Med* **15**, 203-212 (2014). https://doi.org/10.1111/hiv.12105

14 Blackard, J. T. *et al.* HIV mono-infection is associated with FIB-4 - A noninvasive index of liver fibrosis - in women. *Clin Infect Dis* **52**, 674-680 (2011). https://doi.org/10.1093/cid/ciq199

15 Stabinski, L. *et al.* High prevalence of liver fibrosis associated with HIV infection: a study in rural Rakai, Uganda. *Antivir Ther* **16**, 405-411 (2011). https://doi.org/10.3851/IMP1783

16 Tahiri, M. *et al.* Risk factors for liver fibrosis among human immunodeficiency virus monoinfected patients using the FIB4 index in Morocco. *World J Hepatol* **5**, 584-588 (2013). https://doi.org/10.4254/wjh.v5.i10.584

17 Mohsen, A. H. *et al.* Impact of human immunodeficiency virus (HIV) infection on the progression of liver fibrosis in hepatitis C virus infected patients. *Gut* **52**, 1035-1040 (2003). https://doi.org/10.1136/gut.52.7.1035

18 Koyama, Y. & Brenner, D. A. Liver inflammation and fibrosis. *J Clin Invest* **127**, 55-64 (2017). https://doi.org/10.1172/JCI88881

19 Mosoian, A. *et al.* Frontline Science: HIV infection of Kupffer cells results in an amplified proinflammatory response to LPS. *J Leukoc Biol* **101**, 1083-1090 (2017). https://doi.org/10.1189/jlb.3HI0516-242R

20 Zhang, L. *et al.* HIV infection modulates IL-1beta response to LPS stimulation through a TLR4-NLRP3 pathway in human liver macrophages. *J Leukoc Biol* **105**, 783-795 (2019). https://doi.org/10.1002/JLB.4A1018-381R

21 T, L. Analysis of Complex Survey Samples. *journal of Statistical Software*, 1-19 (2004).

22 Panos, A. & Mavridis, D. TableOne: an online web application and R package for summarising and visualising data. *Evid Based Ment Health* **23**, 127-130 (2020). https://doi.org/10.1136/ebmental-2020-300162

23 Alabraba, E. B. *et al.* A new approach to isolation and culture of human Kupffer cells. *J Immunol Methods* **326**, 139-144 (2007). https://doi.org/10.1016/j.jim.2007.06.014

24 Langmead, B. & Salzberg, S. L. Fast gapped-read alignment with Bowtie 2. *Nat Methods* **9**, 357-359 (2012). https://doi.org/10.1038/nmeth.1923

25 Zhang, Y. *et al.* Model-based analysis of ChIP-Seq (MACS). *Genome Biol* **9**, R137 (2008). https://doi.org/10.1186/gb-2008-9-9-r137

26 Li, H. *et al.* The Sequence Alignment/Map format and SAMtools. *Bioinformatics* **25**, 2078-2079 (2009). https://doi.org/10.1093/bioinformatics/btp352

27 Quinlan, A. R. & Hall, I. M. BEDTools: a flexible suite of utilities for comparing genomic features. *Bioinformatics* **26**, 841-842 (2010). https://doi.org/10.1093/bioinformatics/btq033

28 Ramirez, F., Dundar, F., Diehl, S., Gruning, B. A. & Manke, T. deepTools: a flexible platform for exploring deep-sequencing data. *Nucleic Acids Res* **42**, W187-191 (2014). https://doi.org/10.1093/nar/gku365

29 Dobin, A. *et al.* STAR: ultrafast universal RNA-seq aligner. *Bioinformatics* **29**, 15-21 (2013). https://doi.org/10.1093/bioinformatics/bts635

30 Anders, S., Pyl, P. T. & Huber, W. HTSeq--a Python framework to work with high-throughput sequencing data. *Bioinformatics* **31**, 166-169 (2015). https://doi.org/10.1093/bioinformatics/btu638

31 Love, M. I., Huber, W. & Anders, S. Moderated estimation of fold change and dispersion for RNA-seq data with DESeq2. *Genome Biol* **15**, 550 (2014). https://doi.org/10.1186/s13059-014-0550-8

32 Yu, G., Wang, L. G., Han, Y. & He, Q. Y. clusterProfiler: an R package for comparing biological themes among gene clusters. *OMICS* **16**, 284-287 (2012). https://doi.org/10.1089/omi.2011.0118

33 Wu, T. *et al.* clusterProfiler 4.0: A universal enrichment tool for interpreting omics data. *Innovation (Camb)* **2**, 100141 (2021). https://doi.org/10.1016/j.xinn.2021.100141

34 Gennady Korotkevich, V. S., Alexey Sergushichev. Fast gene set enrichment analysis. *bioRaxiv* (2021).

35 Zou, Y. *et al.* The regulatory roles of aminoacyl-tRNA synthetase in cardiovascular disease. *Mol Ther Nucleic Acids* **25**, 372-387 (2021). https://doi.org/10.1016/j.omtn.2021.06.003

36 Kooblall, K. G. *et al.* miR-3156-5p is downregulated in serum of MEN1 patients and regulates expression of MORF4L2. *Endocr Relat Cancer* **29**, 557-568 (2022). https://doi.org/10.1530/ERC-22-0045

37 Becht, D. C. *et al.* MORF and MOZ acetyltransferases target unmethylated CpG islands through the winged helix domain. *Nat Commun* **14**, 697 (2023). https://doi.org/10.1038/s41467-023-36368-5

38 Zimmermann, H. W. *et al.* Interleukin-8 is activated in patients with chronic liver diseases and associated with hepatic macrophage accumulation in human liver fibrosis. *PLoS One* **6**, e21381 (2011). https://doi.org/10.1371/journal.pone.0021381

39 Umemura, T. *et al.* Association between serum soluble CD14 and IL-8 levels and clinical outcome in primary biliary cholangitis. *Liver Int* **37**, 897-905 (2017). https://doi.org/10.1111/liv.13316

40 Ellwanger, J. H. *et al.* Increased IL-8 levels in HIV-infected individuals who initiated ART with CD4(+) T cell counts <350 cells/mm(3) - A potential hallmark of chronic inflammation. *Microbes Infect* **22**, 474-480 (2020). https://doi.org/10.1016/j.micinf.2020.05.019

41 Chen, X. *et al.* Plasma Inflammatory Biomarkers Associated with Advanced Liver Fibrosis in HIV-HCV-Coinfected Individuals. *Int J Environ Res Public Health* **17** (2020). https://doi.org/10.3390/ijerph17249474

42 Keating, S. M. *et al.* The effect of HIV infection and HCV viremia on inflammatory mediators and hepatic injury-The Women's Interagency HIV Study. *PLoS One* **12**, e0181004 (2017). https://doi.org/10.1371/journal.pone.0181004

43 Lang, A. *et al.* Somatostatin inhibits pro-inflammatory cytokine secretion from rat hepatic stellate cells. *Liver Int* **25**, 808-816 (2005). https://doi.org/10.1111/j.1478-3231.2005.01057.x

44 Schwabe, R. F., Schnabl, B., Kweon, Y. O. & Brenner, D. A. CD40 activates NF-kappa B and c-Jun N-terminal kinase and enhances chemokine secretion on activated human hepatic stellate cells. *J Immunol* **166**, 6812-6819 (2001). https://doi.org/10.4049/jimmunol.166.11.6812

45 Paik, Y. H. *et al.* Hepatic stellate cells primed with cytokines upregulate inflammation in response to peptidoglycan or lipoteichoic acid. *Lab Invest* **86**, 676-686 (2006). https://doi.org/10.1038/labinvest.3700422

46 Del Corno, M. *et al.* HIV-1 gp120 signaling through TLR4 modulates innate immune activation in human macrophages and the biology of hepatic stellate cells. *J Leukoc Biol* **100**, 599-606 (2016). https://doi.org/10.1189/jlb.4A1215-534R

47 Takahashi, A., de Andres, M. C., Hashimoto, K., Itoi, E. & Oreffo, R. O. Epigenetic regulation of interleukin-8, an inflammatory chemokine, in osteoarthritis. *Osteoarthritis Cartilage* **23**, 1946-1954 (2015). https://doi.org/10.1016/j.joca.2015.02.168

48 Gatla, H. R. *et al.* Regulation of Chemokines and Cytokines by Histone Deacetylases and an Update on Histone Decetylase Inhibitors in Human Diseases. *Int J Mol Sci* **20** (2019). https://doi.org/10.3390/ijms20051110

49 Roebuck, K. A. Regulation of interleukin-8 gene expression. *J Interferon Cytokine Res* **19**, 429-438 (1999). https://doi.org/10.1089/107999099313866

50 Ashburner, B. P., Westerheide, S. D. & Baldwin, A. S., Jr. The p65 (RelA) subunit of NF-kappaB interacts with the histone deacetylase (HDAC) corepressors HDAC1 and

HDAC2 to negatively regulate gene expression. *Mol Cell Biol* **21**, 7065-7077 (2001). https://doi.org/10.1128/MCB.21.20.7065-7077.2001

51 Vanden Berghe, W., De Bosscher, K., Boone, E., Plaisance, S. & Haegeman, G. The nuclear factor-kappaB engages CBP/p300 and histone acetyltransferase activity for transcriptional activation of the interleukin-6 gene promoter. *J Biol Chem* **274**, 32091-32098 (1999). https://doi.org/10.1074/jbc.274.45.32091

52 Jundi, K. & Greene, C. M. Transcription of Interleukin-8: How Altered Regulation Can Affect Cystic Fibrosis Lung Disease. *Biomolecules* **5**, 1386-1398 (2015). https://doi.org/10.3390/biom5031386

53 Barnes, P. J., Adcock, I. M. & Ito, K. Histone acetylation and deacetylation: importance in inflammatory lung diseases. *Eur Respir J* **25**, 552-563 (2005). https://doi.org/10.1183/09031936.05.00117504

54 Pollicino, T. *et al.* Hepatitis B virus (HBV) induces the expression of interleukin-8 that in turn reduces HBV sensitivity to interferon-alpha. *Virology* **444**, 317-328 (2013). https://doi.org/10.1016/j.virol.2013.06.028

Figure Legends

Figure 1: HIV-1 exposition accentuates the IL-8 response to LTA stimulation in primary isolated HSCs. A) Primary human hepatic stellate cells (pHSCs) were isolated from HIV-uninfected liver tissues (n=3) and treated with LTA (1 μg/ml) either before or after exposition with HIV-1BaL (MOI=0.1) for 48 hours. Supernatants were collected 24 hours after LTA stimulation, and IL-8 levels were measured by ELISA. B) pHSCs from HIV-1-infected liver tissues (n=6) were stimulated with LTA (1 μg/ml) for 24 hours, and IL-8 levels were quantified by ELISA. C) Lx2 cells were treated with LTA alone or HIV-1 plus LTA. Supernatants were collected and IL-8 was measured by ELISA (n=6). D) HIV-1 p24 antigen was quantified by

ELISA in supernatants from HIV-1BaL-exposed Lx2 cells (MOI=0.1) with or without Maraviroc (1 mM) treatment (n=9). E) IL-8 levels were measured by ELISA in HIV-1BaL-exposed Lx2 cells treated with or without Maraviroc (1 mM) (n=6). HIV-1_{BaL}

Figure 2: IL-8 response of HSCs to LTA is independent of the IL-8 and TLR receptor pathways. A) IL-8 receptor was analyzed by Flow cytometry before and after gp120 stimulation (100ng/ml). B) Lx2 cells were stimulated with LTA(1 µg/ml) for 24 hours with or without an IL-8 receptor inhibitor. Supernatants were analyzed for IL-8 levels by ELISA (n=3). C) Lx2 cells were exposed with HIV-1BaL for 48 hours and then treated with either an IL-8 receptor inhibitor or a TLR2 inhibitor. Supernatants were analyzed for IL-8 levels by ELISA (n=3).

Figure 3: Hepatic IL-8 expression is elevated in HIV-1 infected liver tissues alongside enhanced expression of pro-fibrogenic genes. A) Total RNA was extracted from HIV-uninfected (n=7) and HIV-1-infected (n=7) liver tissues. mRNA expression of IL-8, α-SMA, collagen I, and TGF-β was quantified by RT-PCR. B) Protein expression of α-SMA and collagen I was examined by western blot; GAPDH served as a loading control. Band intensity was quantified using ImageJ (n>3). C) IL-8 expression was evaluated by immunohistochemistry in HIV-1 infected and HIV-1 non-infected tissues (n=32). The results were quantified by image J D) Serum IL-8 and LTA concentration were measured in duplicate by ELISA and compared across groups stratified by HIV-1 viremia and fibrosis status ($n^{HIV\text{-}1\ viremia-}$ = 9, $n^{HIV\text{-}1\ viremia-\ Fib+}$ = 9, $n^{HIV\text{-}1\ viremia+Fib+}$ = 10).

Figure 4: IL-8 increases the expression of pro-fibrogenic genes in hepatic stellate cell lines. A) Lx2 cells were treated with increasing concentrations of LTA for 24 hours. mRNA expression of pro-fibrotic and inflammatory genes was quantified by SYBR Green RT-PCR. B) Lx2 cells were repeatedly treated with IL-8 (200 pg/ml) or PBS for 3times. Protein

expression of α-SMA and collagen I was analyzed by western blot and normalized to GAPDH. Band intensities were quantified using ImageJ (n=3).

Figure 5: RNA-seq analysis Suggests a link between histone acetylation and IL-8 Activation following HIV-1 and LTA Co-Stimulation in Lx2 Cells. A-B) Volcano plots showing differentially expressed genes (DEGs) between control, HIV-1_{BaL}-exposed, and HIV-1_{BaL} plus LTA-treated Lx2 cells ($p < 0.05$, $log2FC > 1.0$). Blue and red dots represent up- and down- regulated genes, respectively. C) Heatmap analysis of inflammatory genes across treatment groups. D) ClueGO pathway enrichment of genes positively correlated with IL-8 expression (correlation coefficient > 0.2), highlighting the tRNA aminoacylation pathway. E) Cytoscape-based network reconstruction of the tRNA aminoacylation pathway, showing CXCL8 (IL-8) enrichment. F) Heatmap of tRNA aminoacylation gene expression across the three conditions. G) Heatmap analysis of Acetylation related genes across the three conditions.

Figure 6: H4K5 Acetylation is Essential for IL-8 Response to LTA stimulation in HIV-1 infected HSCs. A) Two pHSCs isolated from HIV-1 negative individuals were stimulated with LTA with or without HDAC inhibitor (TSA) for 24hrs, IL-8 in supernatant was measured by ELISA (n=6). B) Two pHSCs isolated from HIV-1 infected individuals were stimulated with LTA with or without HDAC inhibitor (TSA) for 24hrs, IL-8 in supernatant was measured by ELISA (n=6). C) H4K5 acetylation protein was measured by ELISA in both pHSCs (n=4) and Lx2 cell lines (n=8) before and after HIV-1_{BaL} exposition. D) H4K5 acetylation protein was examined by western blotting and normalized to GAPDH. E) Binding motif analysis of IL-8 promoter. F) Chromatin immunoprecipitation (ChIP) was performed using anti-H4K5 antibody. DNA was purified and analyzed by SYBR RT-PCR for enrichment of NF-κB, AP-1, and NF-IL6 binding motifs in the IL-8 promoter.

Tables

Table 1: Primers:

All primer sequences.

h-a-SMA R: 5’-AGGCACCCCTGAACCCCAA-3'
h-a-SMA R: 5’-CAGCACCGCCTGGATAGCC-3’
h-Collagen I F: 5’-GGCTTCCCTGGTCTTCCTGG-3’
h-Collagen I R: 5’-CCAGGGGGTCCAGCCAAT-3’
h-PDGF F: 5’-CCAGAAGCCATCAGCAGCAAG-3’
h-PDGF R: 5’-AGGCCCTGAGAGATCTGTGG-3’
h-MMP2 F: 5’- CCCCAAGCTCATCGCAGAT-3’
h-MMP2 R: 5’- GGTCCACGACGGCATCC-3’
h-TIMP1 F: 5′-TGACATCCGGTTCGTCTACA-3′
h-TIMP1 R: 5′-TGATGTGCAAGAGTCCATCC-3′
h-TIMP2 F: 5’- AAGCGGTCAGTGAGAAGGAA-3’
h-TIMP2 R: 5′-GGGGGCCGTGTAGATAAACT-3′
h-TGF-beta F: 5’-CAAGGGCTACCATGCCAACT-3’
h-TGF-beta R: 5’-AGGGCCAGGACCTTGCTG-3’
h-TGF-beta1 Receptor F: 5′-CGACTGCCAAATGAAGAGGACC-3′
h-TGF-beta1 Receptor R: 5′-AAACCTGAGCCAGAACCTGACG-3′
h-IL-8 F: 5'-TAGGACAAGAGCCAGGAAGA-3'
h-IL-8R: 5'-CTTCCTGATTTCTGCAGCTCT-3'
h-GAPDH F: 5'-CAATGACCCCTTCATTGACC-3’
h-GAPDH R: 5'- GACAAGCTTCCCGTTCTCAG -3'

Table 2: Characteristics of blood donors

	Overall	0	1	p test
n	28	11	17	
Sigfibrosis = 1 (%)	17.0 (60.7)	0.0 (0.0)	17.0 (100.0)	<0.001
gender = 2 (%)	5.0 (17.9)	2.0 (18.2)	3.0 (17.6)	0.972
Ethinic (%)				0.368
AA	7.0 (25.0)	2.0 (18.2)	5.0 (29.4)	
AS	1.0 (3.6)	0.0 (0.0)	1.0 (5.9)	
HS	13.0 (46.4)	4.0 (36.4)	9.0 (52.9)	
O	3.0 (10.7)	2.0 (18.2)	1.0 (5.9)	
W	4.0 (14.3)	3.0 (27.3)	1.0 (5.9)	
age (mean (SD))	52.89 (9.52)	53.55 (4.27)	52.47 (11.88)	0.732
bmi (mean (SD))	30.55 (6.62)	29.21 (6.42)	31.41 (6.79)	0.384

alcohol = 1 (%)	9.0 (32.1)	3.0 (27.3)	6.0 (35.3)	0.666
duradiag (mean (SD))	19.82 (8.69)	19.20 (8.94)	20.33 (8.85)	0.762
viremia = 1 (%)	19.0 (67.9)	11.0 (100.0)	8.0 (47.1)	0.005
cd4 (mean (SD))	649.18 (324.81)	627.00 (348.98)	663.53 (318.36)	0.777
fibroscan (mean (SD))	9.33 (5.21)	5.50 (1.23)	11.81 (5.31)	<0.001
plt (mean (SD))	197.71 (63.29)	200.73 (58.45)	195.76 (67.93)	0.835
alt (mean (SD))	30.46 (20.36)	23.00 (9.14)	35.29 (24.17)	0.065
ALTab = 1 (%)	10.0 (35.7)	2.0 (18.2)	8.0 (47.1)	0.138
alp (mean (SD))	91.18 (28.40)	82.55 (34.78)	96.76 (22.82)	0.23
alb (mean (SD))	3.86 (0.82)	4.01 (0.29)	3.77 (1.02)	0.366
fbs (mean (SD))	106.61 (37.03)	90.45 (22.32)	117.06 (41.31)	0.034
chol (mean (SD))	167.71 (41.52)	182.73 (48.59)	158.00 (34.33)	0.144
tg (mean (SD))	167.79 (133.44)	170.91 (122.65)	165.76 (143.64)	0.918
hdl (mean (SD))	41.78 (9.67)	42.20 (9.37)	41.53 (10.12)	0.86
lowHDL (mean (SD))	0.56 (0.51)	0.50 (0.53)	0.59 (0.51)	0.666
ldl (mean (SD))	94.18 (34.95)	110.04 (45.12)	83.92 (22.46)	0.079
CAP (mean (SD))	283.18 (61.62)	261.00 (66.65)	297.53 (55.45)	0.134
fattyliver = 1 (%)	23.0 (82.1)	8.0 (72.7)	15.0 (88.2)	0.313
AST (mean (SD))	28.38 (12.35)	25.27 (10.58)	30.67 (13.39)	0.253
HCV (mean (SD))	0.46 (0.51)	0.45 (0.52)	0.47 (0.51)	0.936
HBV (mean (SD))	0.04 (0.19)	0.00 (0.00)	0.06 (0.24)	0.321
HSI (mean (SD))	37.48 (13.26)	37.87 (7.23)	37.21 (16.43)	0.886
FIB4 (mean (SD))	1.67 (1.24)	1.59 (0.86)	1.74 (1.48)	0.738

Definition:

Active alcohol consumption = drinking more than 10 g of ethanol per day in females and 20 g per day in males

Liver steatosis = evidence of CAP more than 248 dB/m

Figure 1

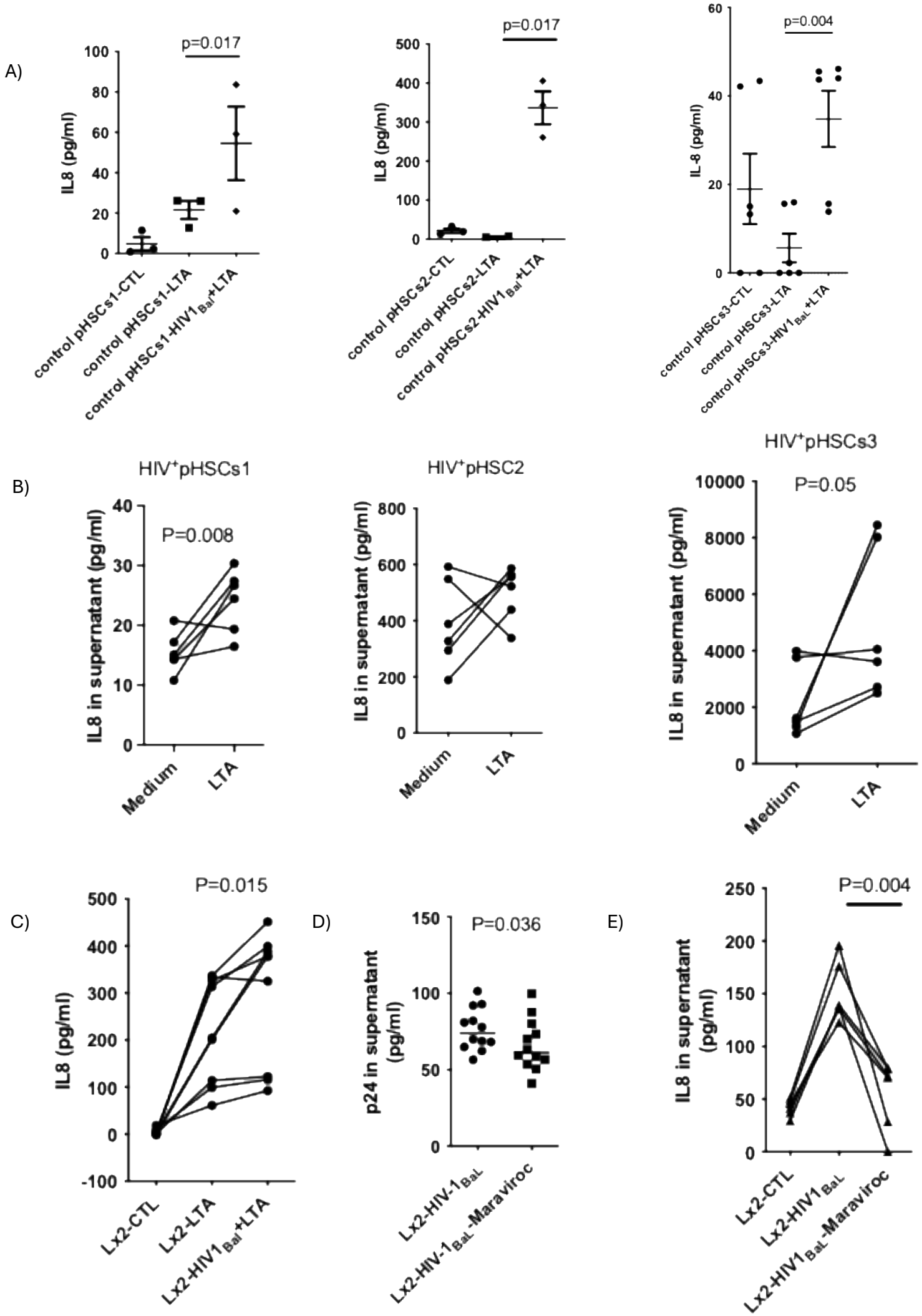
A)
p=0.017
IL8 (pg/ml)
control pHSCs1-CTL
control pHSCs1-LTA
control pHSCs1-HIV1BaL+LTA
p=0.017
IL8 (pg/ml)
control pHSCs2-CTL
control pHSCs2-LTA
control pHSCs2-HIV1BaL+LTA
p=0.004
IL-8 (pg/ml)
control pHSCs3-CTL
control pHSCs3-LTA
control pHSCs3-HIV1BaL+LTA
B)
HIV+pHSCs1
P=0.008
IL8 in supernatant (pg/ml)
Medium
LTA
HIV+pHSC2
IL8 in supernatant (pg/ml)
Medium
LTA
HIV+pHSCs3
P=0.05
IL8 in supernatant (pg/ml)
Medium
LTA
C)
P=0.015
IL8 (pg/ml)
Lx2-CTL
Lx2-LTA
Lx2-HIV1BaL+LTA
D)
P=0.036
p24 in supernatant (pg/ml)
Lx2-HIV-1BaL
Lx2-HIV-1BaL-Maraviroc
E)
P=0.004
IL8 in supernatant (pg/ml)
Lx2-CTL
Lx2-HIV1BaL
Lx2-HIV1BaL-Maraviroc

Figure 2

A)

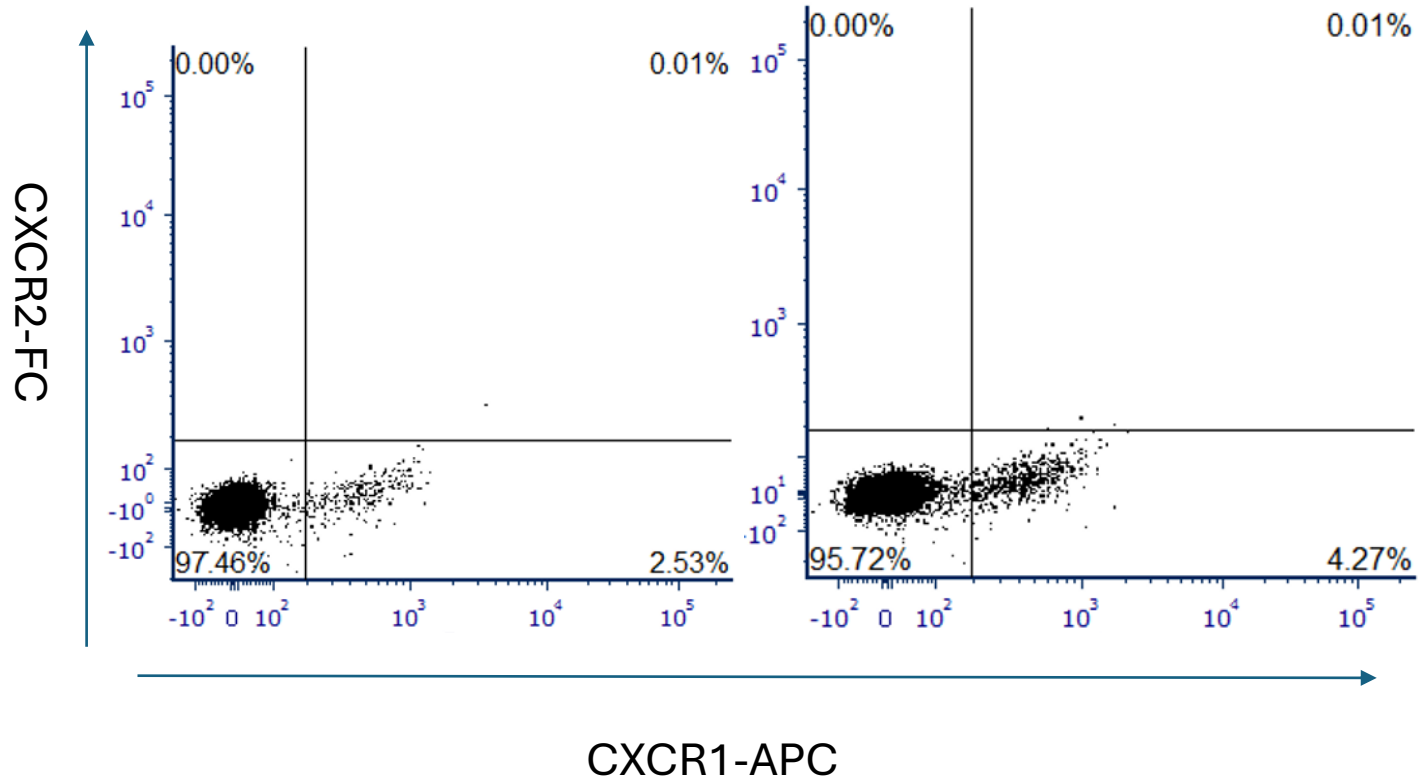
CXCR2-FC
0.00%
0.01%
97.46%
2.53%
0.00%
0.01%
95.72%
4.27%
CXCR1-APC

B)

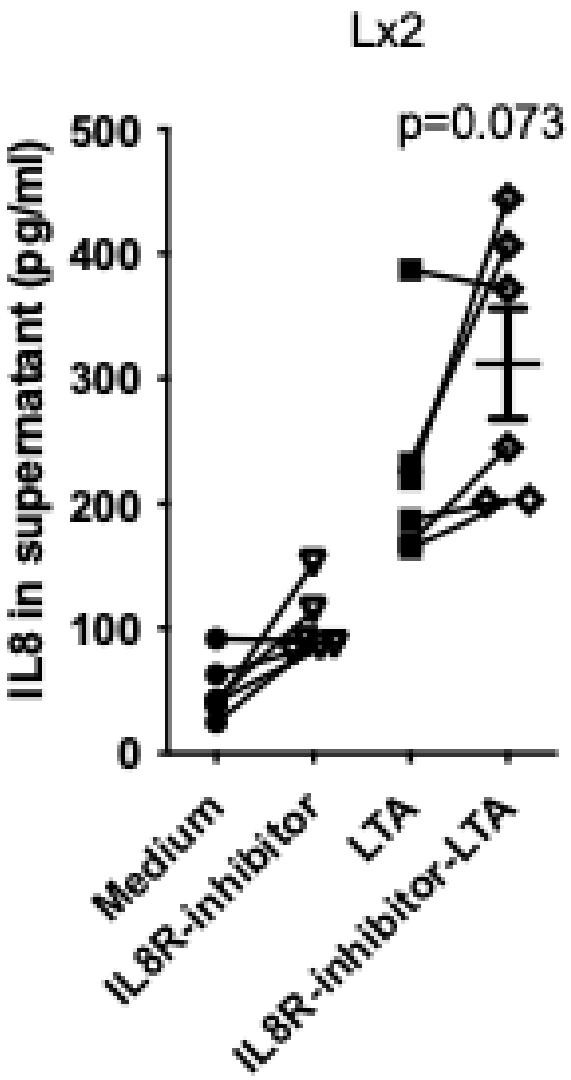
Lx2
p=0.073
IL8 in supernatant (pg/ml)
500
400
300
200
100
0
Medium
IL8R-inhibitor
LTA
IL8R-inhibitor-LTA

C)

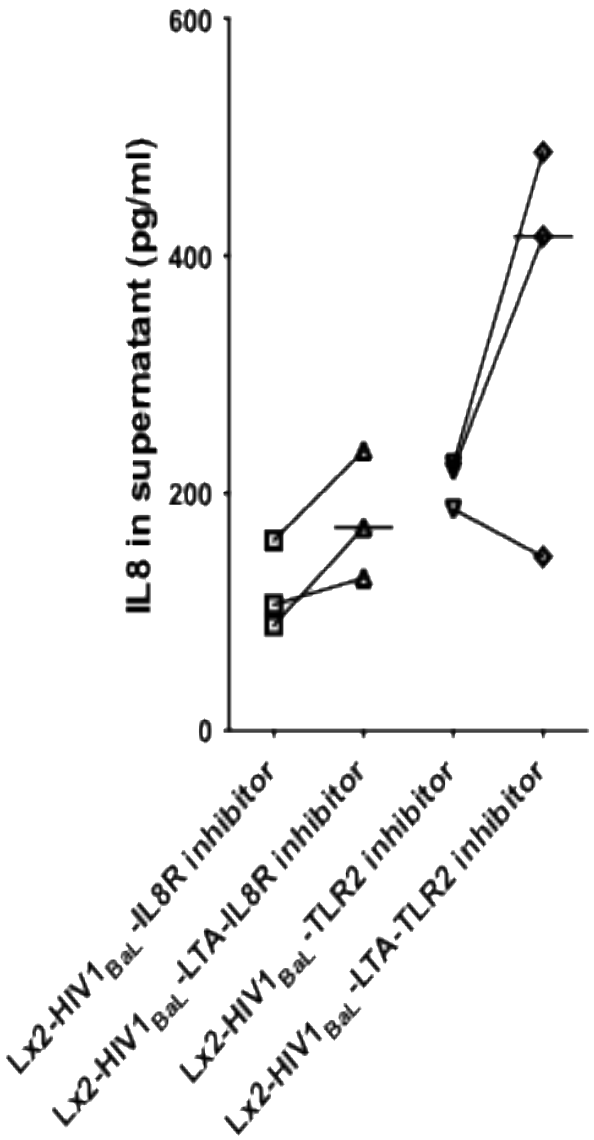
IL8 in supernatant (pg/ml)
600
400
200
0
Lx2-HIV1BaL -IL8R inhibitor
Lx2-HIV1BaL -LTA-IL8R inhibitor
Lx2-HIV1BaL -TLR2 inhibitor
Lx2-HIV1BaL -LTA-TLR2 inhibitor

Figure 3

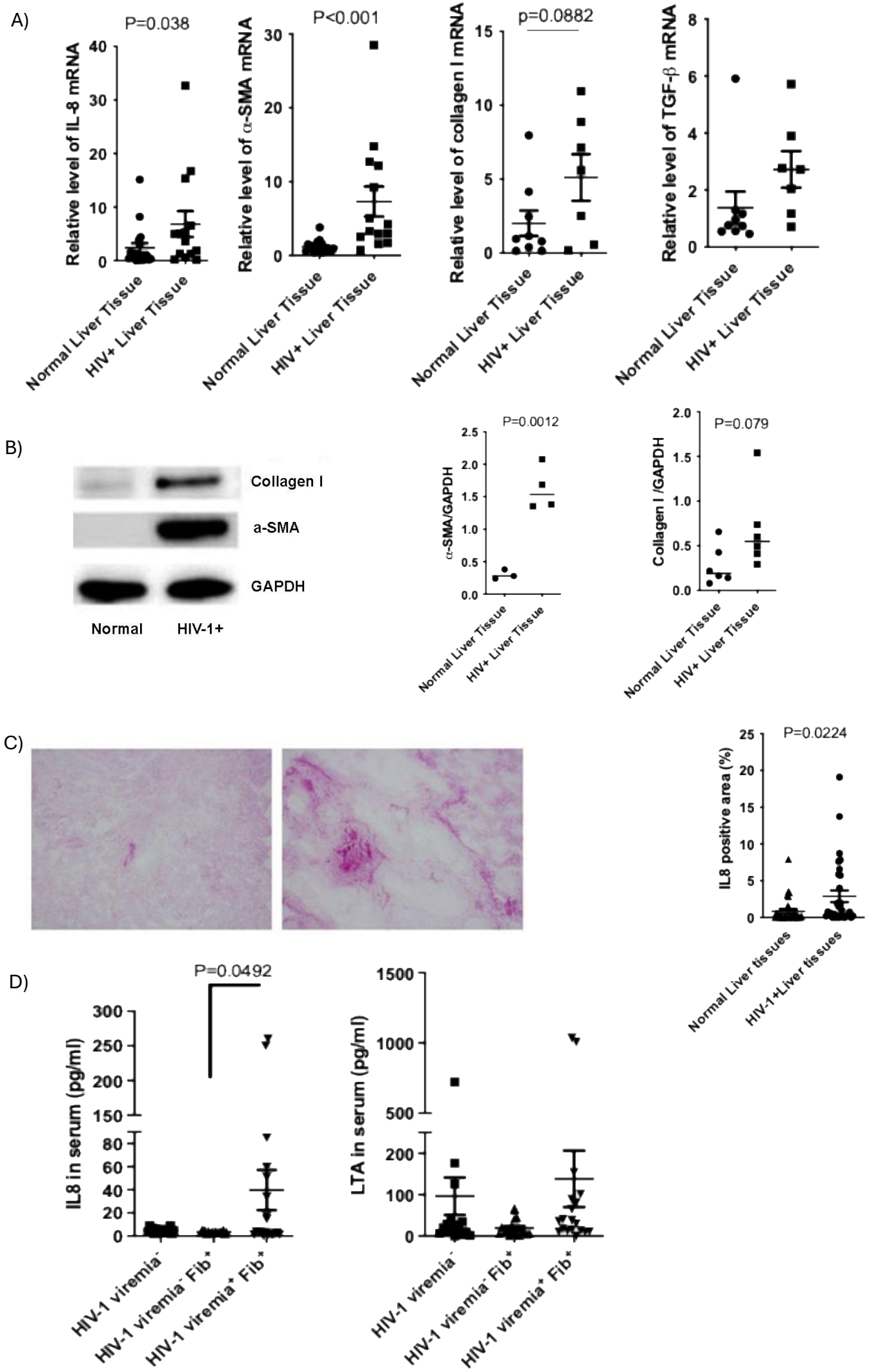
A)
P=0.038
Relative level of IL-8 mRNA
P<0.001
Relative level of α-SMA mRNA
p=0.0882
Relative level of collagen I mRNA
Relative level of TGF-β mRNA
Normal Liver Tissue
HIV+ Liver Tissue
B)
Collagen I
a-SMA
GAPDH
Normal
HIV-1+
P=0.0012
α-SMA/GAPDH
P=0.079
Collagen I /GAPDH
C)
P=0.0224
IL8 positive area (%)
Normal Liver tissues
HIV-1+Liver tissues
D)
P=0.0492
IL8 in serum (pg/ml)
LTA in serum (pg/ml)
HIV-1 viremia⁻
HIV-1 viremia⁻ Fib⁺
HIV-1 viremia⁺ Fib⁺

Figure 4

A)

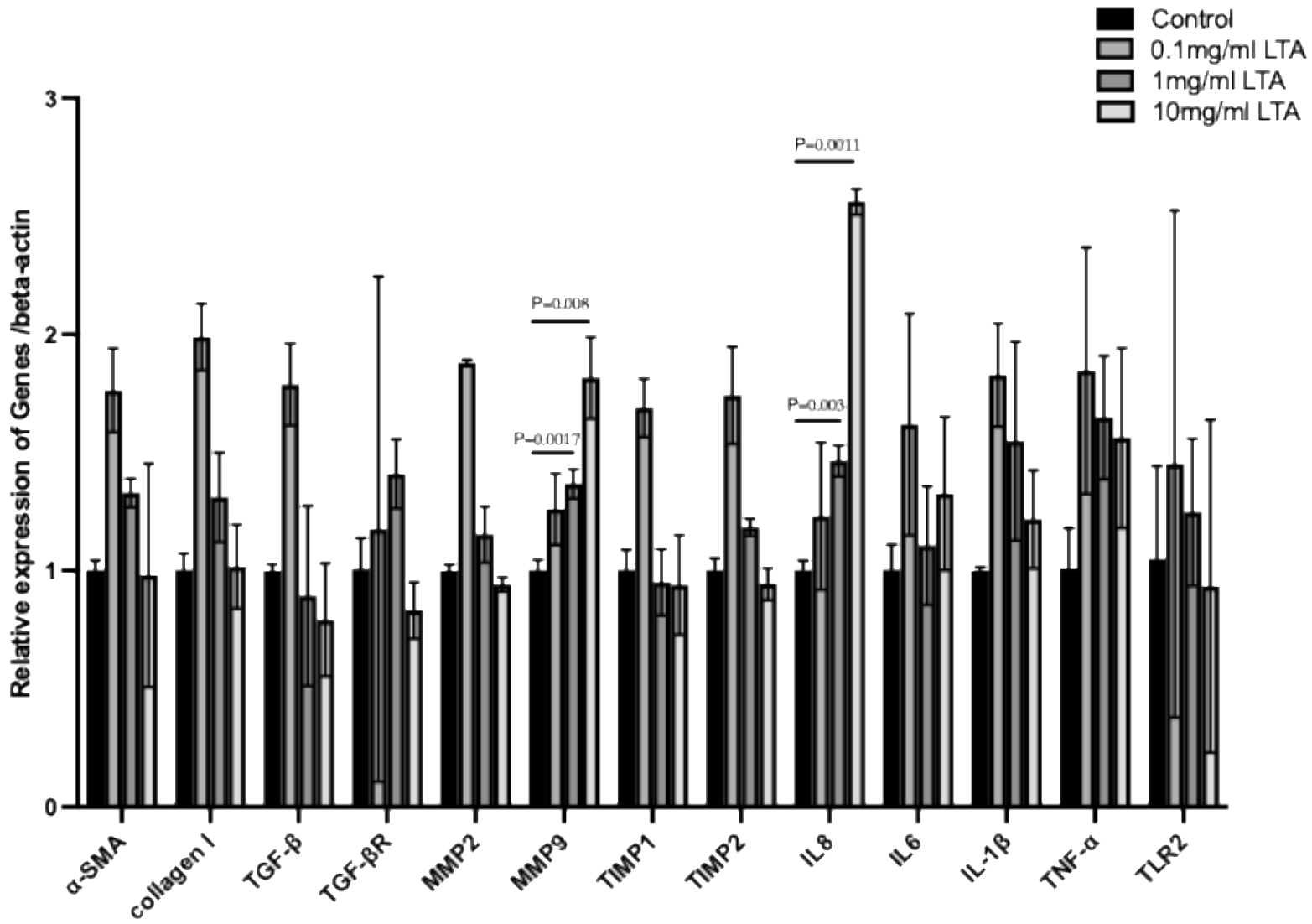
Control
0.1mg/ml LTA
1mg/ml LTA
10mg/ml LTA
Relative expression of Genes /beta-actin
3
2
1
0
P=0.0011
P=0.008
P=0.0017
P=0.003
α-SMA
collagen I
TGF-β
TGF-βR
MMP2
MMP9
TIMP1
TIMP2
IL8
IL6
IL-1β
TNF-α
TLR2

B)

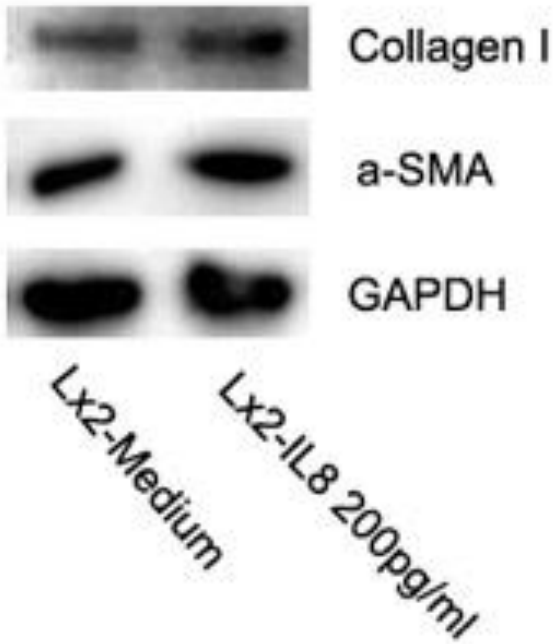
Collagen I
a-SMA
GAPDH
Lx2-Medium
Lx2-IL8 200pg/ml

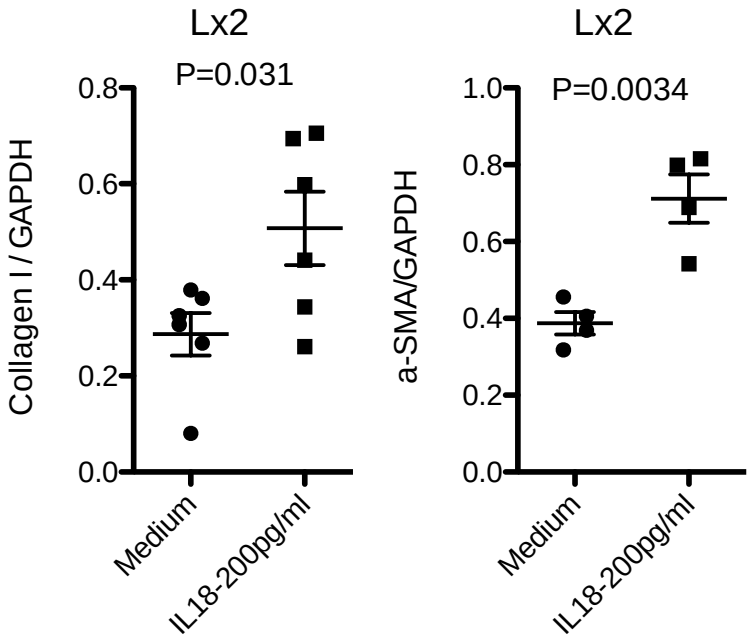
Lx2
P=0.031
Collagen I / GAPDH
0.8
0.6
0.4
0.2
0.0
Medium
IL18-200pg/ml
Lx2
P=0.0034
a-SMA/GAPDH
1.0
0.8
0.6
0.4
0.2
0.0
Medium
IL18-200pg/ml

Figure 5

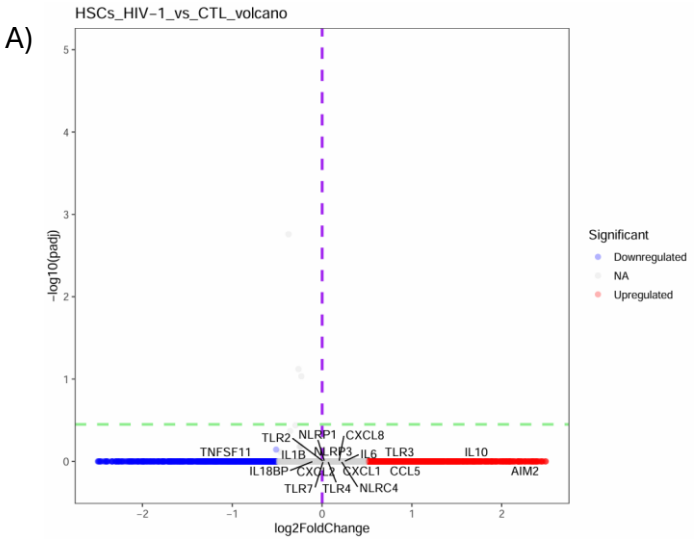
A)
HSCs_HIV-1_vs_CTL_volcano
-log10(padj)
log2FoldChange
Significant
Downregulated
NA
Upregulated
TLR2
NLRP1
CXCL8
TNFSF11
IL1B
NLRP3
IL6
TLR3
IL10
IL18BP
CXCL2
CXCL1
CCL5
AIM2
TLR7
TLR4
NLRC4

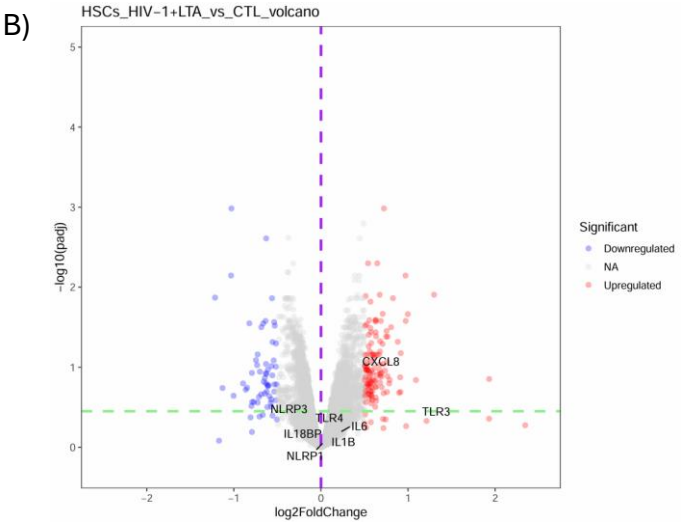
B)
HSCs_HIV-1+LTA_vs_CTL_volcano
-log10(padj)
log2FoldChange
Significant
Downregulated
NA
Upregulated
CXCL8
NLRP3
TLR4
IL6
TLR3
IL18BP
IL1B
NLRP1

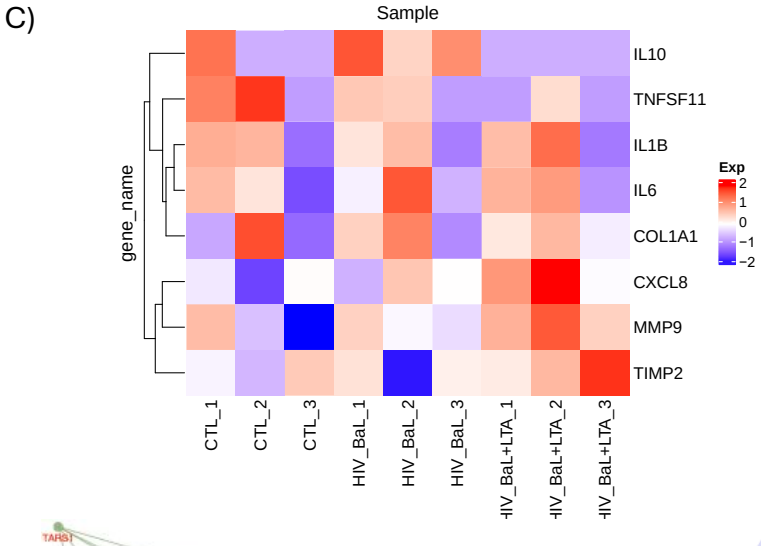
C)
Sample
gene_name
IL10
TNFSF11
IL1B
IL6
COL1A1
CXCL8
MMP9
TIMP2
Exp
CTL_1
CTL_2
CTL_3
HIV_BaL_1
HIV_BaL_2
HIV_BaL_3
HIV_BaL+LTA_1
HIV_BaL+LTA_2
HIV_BaL+LTA_3

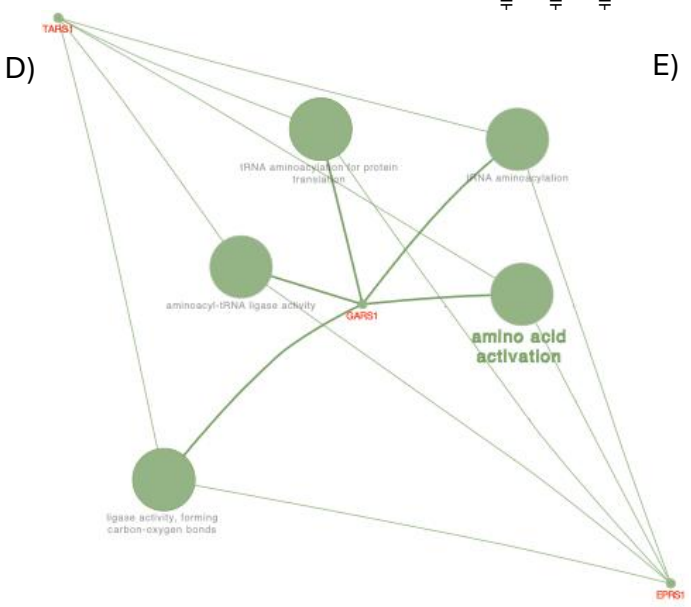
D)
TARS1
tRNA aminoacylation for protein translation
tRNA aminoacylation
aminoacyl-tRNA ligase activity
GARS1
amino acid activation
ligase activity, forming carbon-oxygen bonds
EPRS1

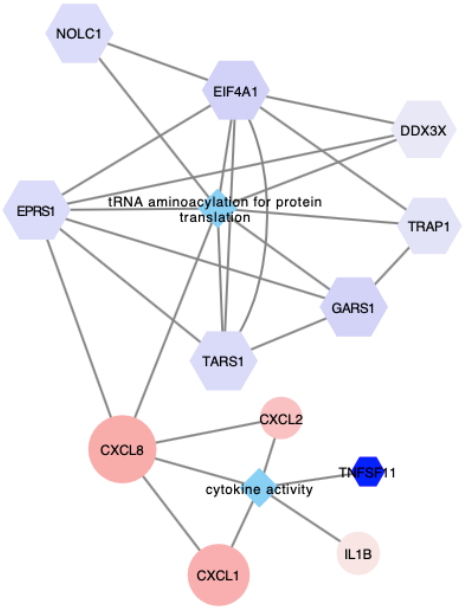
E)
NOLC1
EIF4A1
DDX3X
EPRS1
tRNA aminoacylation for protein translation
TRAP1
GARS1
TARS1
CXCL2
CXCL8
TNFSF11
cytokine activity
IL1B
CXCL1

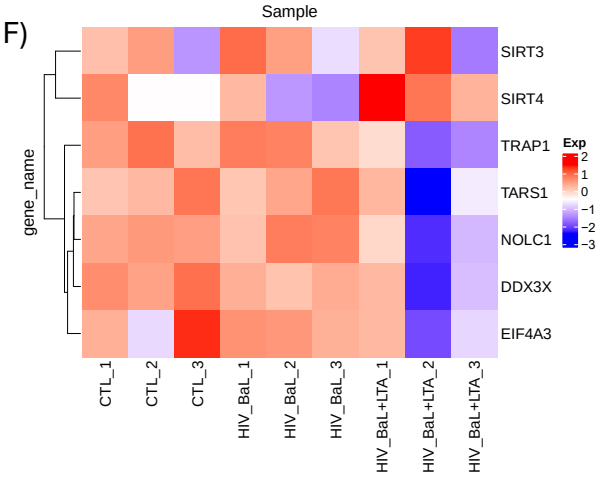
F)
Sample
gene_name
SIRT3
SIRT4
TRAP1
TARS1
NOLC1
DDX3X
EIF4A3
Exp
CTL_1
CTL_2
CTL_3
HIV_BaL_1
HIV_BaL_2
HIV_BaL_3
HIV_BaL+LTA_1
HIV_BaL+LTA_2
HIV_BaL+LTA_3

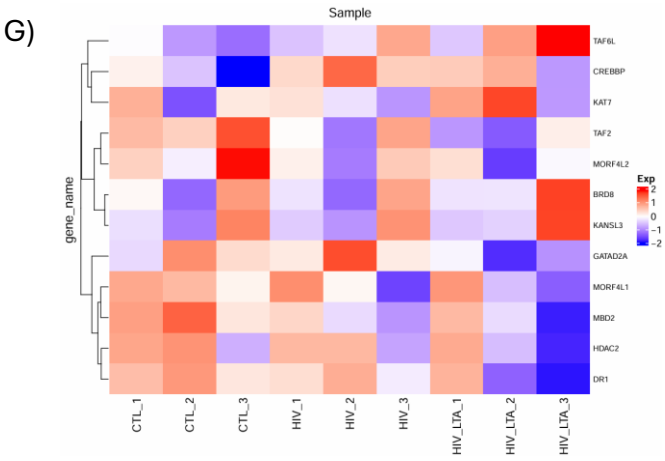
G)
Sample
gene_name
TAF6L
CREBBP
KAT7
TAF2
MORF4L2
BRD8
KANSL3
GATAD2A
MORF4L1
MBD2
HDAC2
DR1
Exp
CTL_1
CTL_2
CTL_3
HIV_1
HIV_2
HIV_3
HIV_LTA_1
HIV_LTA_2
HIV_LTA_3

Figure 6

A)

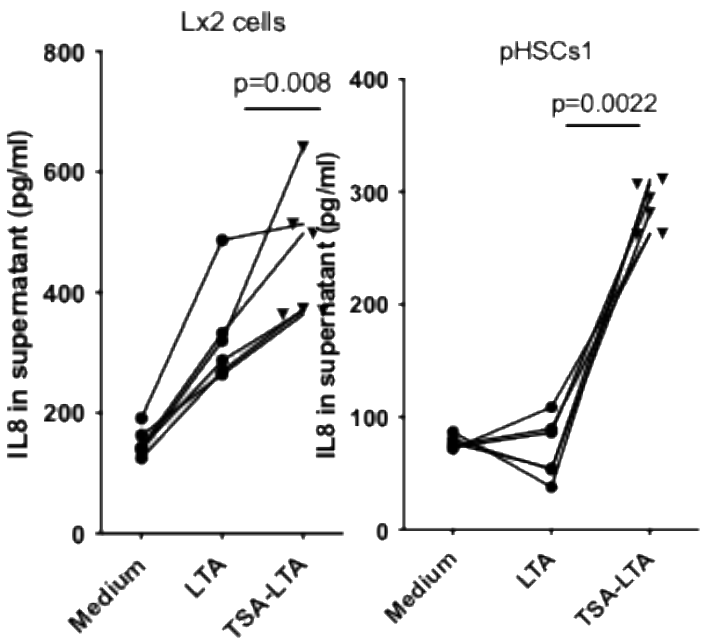

B)

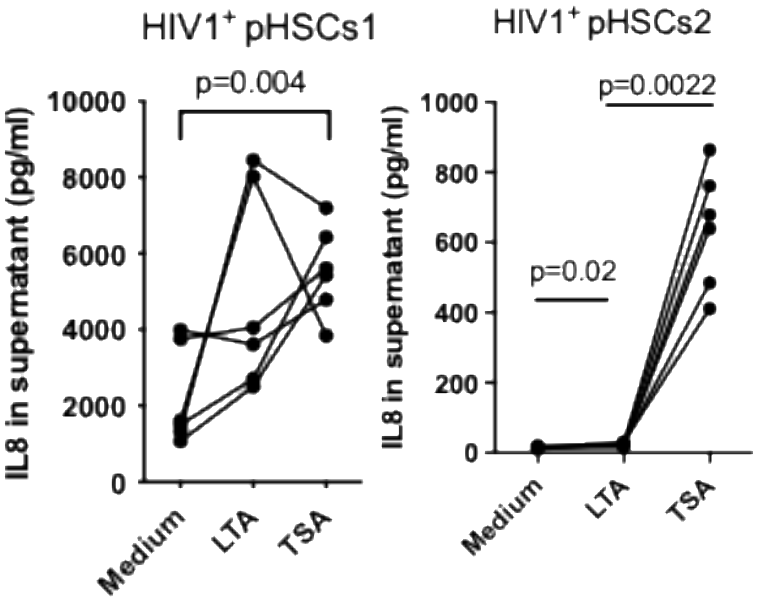

C)

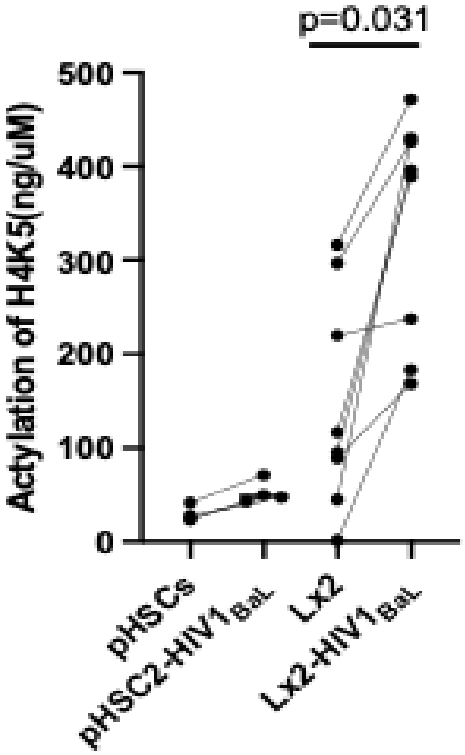

D)

E)

TGGAACCCAGATGCTCTTTCCACTAAGCATACAACTTTCCATTAGATAACACCTCCCTCCCACCCCAACCA
AGCAGCTCCAGTGCACCACTTTCTGGAGCATAAACATACCTTAACTTTACAACTTGAGTGGCCTTGAATAC
TGTTCCTATCTGGAATGTGCTGTTCTCTTTCATCTTCCTCTATTGAAGCCCTCCTATTCCTCAATGCCTTG
CTCCAACTGCCTTTGGAAGATTCTGCTCTTATGCCTCCACTGGAATTAATGTCTTAGTACCACTTGTCTAT
TCTGCTATATAGTCAGTCCTTACATTGCTTTCTTCTTCTGATAGACCAAACTCTTTAAGGACAAGTACCTA
GTCTTATCTATTTCTAGATCCCCCACATTACTCAGAAAGTTACTCCATAAATGTTTGTGGAACTGATTTCT
ATGTGAAGCACATGTGCCCCTTCACTCTGTTAACATGCATTAGAAAACTAAATCTTTTGAAAAGTTGTAGT
ATGCCCCCTAAGAGCAGTAACAGTTCCTAGAAACTCTCTAAAATGCTTAGAAAAAGATTTATTTTAAATTA
CCTCCCCAATAAAATGATTGGCTGGCTTATCTTCACCATCATGATAGCATCTGTAATTAACTGAAAAAAAA
TAATTATGCCATTAAAAGAAAATCATCCATGATCTTGTTCTAACACCTGCCACTCTAGTACTATATCTGTC
ACATGGTACTATGATAAAGTTATCTAGAAATAAAAAAGCATACAATTGATAATTCACCAAATTGTGGAGCT
TCAGTATTTTAAATGTATATTAAAATTAAATTATTTTAAAGATCAAAGAAAACTTTCGTCATACTCCGTAT
TTGATAAGGAACAAATAGGAAGTGTGATGACTCAGGTTTGCCCTGAGGGGATGGGCCATCAGTTGCAAATC
GTGGAATTTCCTCTGACATAATGAAAAGATGAGGGTGCATAAGTTCTCTAGTAGGGTGATGATATAAAAAG
CCACCGGAGCACTCCATAAGGCACAAACTTTCAGAGACAGCAGAGCACACAAGCTTCTAGGACAAGAGCCA
GGAAGAAACCACCGGAAGGAACCATCTCACTGTGTGTAAACAT

Red Bold : NF-IL16:
Purple Bold : AP-1
Blue Bold : NF-kB
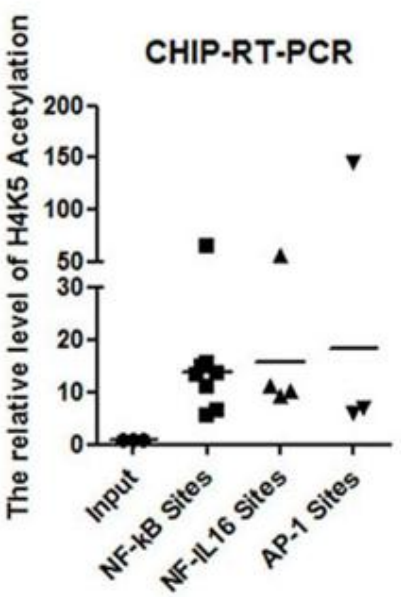
F)